

Entrapment of Chromosomes by Condensin Rings Prevents their Breakage During Cytokinesis

Sara Cuylen,^{1,2,3} Jutta Metz,^{1,2} Andrea Hruby,^{1,2} and Christian H. Haering^{1,2,*}

¹Cell Biology & Biophysics Unit and ²Structural & Computational Biology Unit, European Molecular Biology Laboratory (EMBL), Meyerhofstraße 1, 69117 Heidelberg, Germany

³Present address: Institute of Molecular Biotechnology (IMBA), Dr. Bohr-Gasse 3, 1030 Vienna, Austria

*Correspondence: christian.haering@embl.de

This is the unedited version of the manuscript published in final form in *Developmental Cell* Volume 27, Issue 4, 469-478, 25 November 2013

SUMMARY

Successful segregation of chromosomes during mitosis and meiosis depends on the action of the ring-shaped condensin complex, yet how condensin ensures the complete disjunction of sister chromatids is unknown. We show that the failure to segregate chromosome arms, which results from condensin release from chromosomes by proteolytic cleavage of its ring structure, leads to a DNA damage checkpoint-dependent cell cycle arrest. Checkpoint activation is triggered by the formation of chromosome breaks during cytokinesis, which proceeds with normal timing despite the presence of lagging chromosome arms. Remarkably, enforcing condensin ring re-closure by chemically induced dimerization just before entry into anaphase is sufficient to restore chromosome arm segregation. We suggest that topological entrapment of chromosome arms by condensin rings ensures their clearance from the cleavage plane and thereby avoids their breakage during cytokinesis.

RESEARCH HIGHLIGHTS

- Disrupting condensin ring integrity results in chromosome arm missegregation
- Cell division proceeds despite the presence of chromatin at the cleavage plane
- Breakage of chromosomes during cytokinesis triggers the DNA damage pathway
- Condensin ring re-closure is sufficient to restore anaphase segregation

INTRODUCTION

Condensin complexes play central roles for the successful segregation of chromosomes during mitotic and meiotic cell divisions (reviewed by [Piazza et al., 2013](#)). While the effects of depletion or mutation of condensin subunits on the proper folding of mitotic chromosomes vary between model systems, chromosomes that lack condensin predominantly fail to partition correctly during anaphase (reviewed by [Hirano, 2012](#)). The molecular mechanisms by which condensin prevents lagging or bridged chromosomes have remained poorly understood. One option is that condensin, together with topoisomerase II (topo II), actively participates in the decatenation of entangled sister chromatids and thereby enables their complete separation ([Baxter et al., 2011](#)). This function might be particularly important at repetitive chromosome regions such as, for example, the ribosomal DNA repeats in budding yeast ([D'Ambrosio et al., 2008](#); [D'Amours et al., 2004](#)). Alternatively, condensin might be required to generate a recoiling force that promotes the removal of residual sister chromatid cohesion ([Renshaw et al., 2010](#)). Yet another hypothesis envisions that condensin functions as a molecular linker that connects different parts of a chromosome and thereby assists in chromatid resolution (discussed in [Cuylen and Haering, 2011](#)).

Surprisingly little is known about how cells deal with the chromosome segregation failures that result from deficiencies in condensin function. Lagging or non-disjoined chromosomes present evidently an obstacle for cytokinesis. In animal cells, chromosome bridges frequently result in the abortion of cytokinesis and the formation of tetraploid cells ([Mullins and Biesele, 1977](#); [Shi and King, 2005](#)); an event that has been shown to promote tumorigenesis ([Fujiwara et al., 2005](#)). Recent work demonstrated that Aurora B kinase activity delays abscission in cells with chromosome bridges, most likely to allow resolution of the bridges and to prevent tetraploidization due to cleavage furrow regression ([Carlton et al., 2012](#); [Steigemann et al., 2009](#)). Condensin I, which co-localizes with Aurora B to chromosome bridges, might play a crucial role in this process ([Bembenek et al., 2013](#)). Despite this surveillance mechanism, chromosomes that failed to segregate get frequently damaged during cytokinesis ([Gascoigne and Cheeseman, 2013](#); [Janssen et al., 2011](#)). A similar Aurora kinase-dependent mechanism has been suggested to prevent severance of non-segregated chromosomes during cytokinesis in budding yeast ([Mendoza et al., 2009](#); [Norden et al., 2006](#)). Other studies, however, report that cell division proceeds even in the presence of non-disjoined chromatin masses in budding ([Baxter and Diffley, 2008](#); [McGrew et al., 1992](#)) and fission yeasts (to produce a so-called 'cut' phenotype; [Hirano et al., 1986](#)).

We recently discovered that condensin complexes topologically entrap chromosomal DNAs within the large ring-shaped

structure formed by their Structural maintenance of chromosomes (Smc2–Smc4) and kleisin (Brn1) subunits ([Cuylen et al., 2011](#)). Release of condensin from chromosomes in live budding yeast cells by ring opening through site-specific cleavage of Brn1 with Tobacco Etch Virus (TEV) protease has no effect on the partitioning of the centromeres of a model chromosome (chromosome V) but frequently prevents the segregation of the arm of the same chromosome into the daughter cell. Here, we investigate the consequences that arise from the persistence of chromosome arms at the cytokinetic cleavage plane after condensin release.

RESULTS

Condensin Cleavage Induces a DNA Damage Checkpoint-Dependent Cell Cycle Arrest

To investigate the consequences of chromosome arm segregation failure after condensin release from chromosomes, we opened condensin rings by TEV-mediated Brn1 cleavage in yeast cells that had been arrested in metaphase by depletion of the Anaphase Promoting Complex/Cyclosome (APC/C) activator Cdc20. We then released the cells from the arrest by Cdc20 re-induction and recorded their progression through the cell cycle by live cell microscopy in a microfluidic flow chamber for more than 12 h. Surprisingly, despite chromosome segregation defects, more than 85% of cells with cleaved condensin rings exited mitosis and entered a new cell cycle ([Figure 1A](#)). However, nearly all of these cells then arrested as large-budded cells for the remainder of the time course ([Figure 1B](#)). Cells with intact condensin rings in contrast underwent in average 5-6 divisions during the period of imaging ([Figure 1A](#)). This suggests that most cells that undergo mitosis with cleaved condensin rings are blocked in the following G2 or M phases.

To determine more precisely at which stage of the cell cycle cells with cleaved condensin rings arrest, we monitored mitotic spindle dynamics in cells expressing GFP-labeled tubulin. Cells with intact Brn1 underwent anaphase within ~30 min ([Figure 1C](#) and [Movie S1](#) in the Supplemental Data available with this article online) and entered the next cell cycle within ~60 min after release from metaphase, as judged by bud formation ([Figure 1D](#)). 95% of these cells then assembled a new metaphase spindle and initiated a second anaphase within the next 160 min ([Figure 1E](#)). The majority of cells released from the metaphase arrest with cleaved condensin rings completed the first anaphase, entered the next cell cycle, and assembled a new metaphase spindle with a similar timing as cells with intact condensin rings. However, these cells then failed to initiate a second anaphase and instead remained arrested with a metaphase spindle until the end of the time course ([Figures 1D-F](#) and [Movie S1](#)).

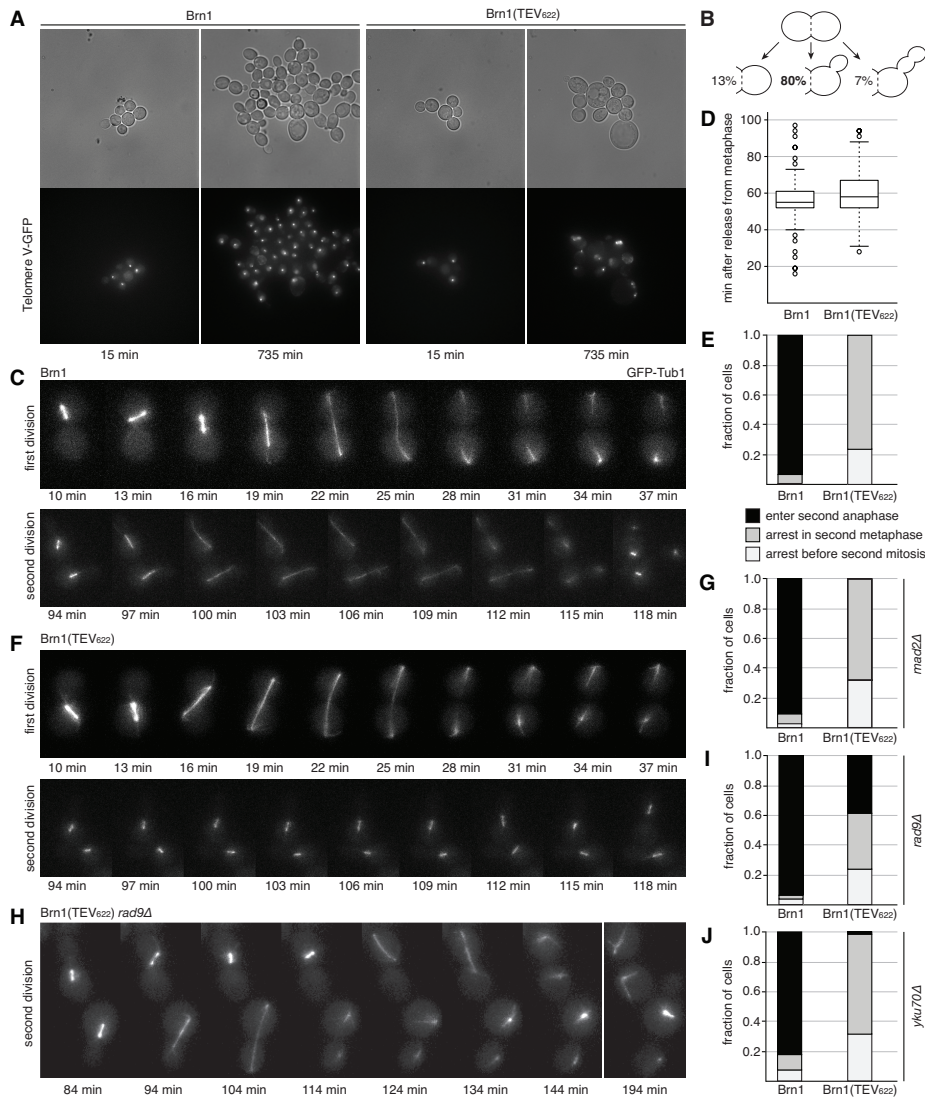


Figure 1. Condensin release from chromosomes results in a DNA damage pathway-dependent cell cycle arrest

(A-B) Cell division and segregation of a GFP marker array integrated proximal to the right telomere of chromosome V were monitored for 12.25 h in a microfluidic flow cell of cells released from metaphase with intact (strain C2513) or TEV-cleaved (strain C2618) Brn1. The fraction of cells that did not form buds, budded once, or re-budded a second time was scored (n = 69 cells).

(C) Mitotic spindle dynamics were recorded of a cell released from metaphase with intact condensin (strain C3257).

(D) The time between release from metaphase arrest and bud formation was scored for cells with intact or cleaved condensin (strains C3257 and C3258). Data represent the median (line), the 25th, 75th (boxes), 5th and 95th percentile (whiskers) (n = 69-114 cells).

(E) The fractions of cells from (C and F) that failed to form a new mitotic spindle, arrested with a metaphase spindle, or underwent a second anaphase spindle extension within 190 min after release from metaphase were scored (n ≥ 130 cells).

(F) Mitotic spindle dynamics of a cell with cleaved Brn1 (strain C3258) was monitored as in (C).

(G) Passage through mitosis of *mad2Δ* cells (strains C3279 and C3280) was scored as in (E) (n > 110 cells).

(H) Mitotic spindle dynamics of a *rad9Δ* cell with cleaved Brn1 (strain C3512) was monitored as in (C).

(I) Passage through mitosis of *rad9Δ* cells (strains C3467 and C3512) was scored as in (E) (n > 120 cells).

(J) Passage through mitosis of *yku70Δ* cells (strains C3873 and C3874) was scored as in (E) (n > 95 cells).

See also [Movies S1](#) and [S2](#).

A plausible cause for the arrest in metaphase might be a defect in the attachment of kinetochores to mitotic spindle microtubules after condensin release from chromosomes (Brito et al., 2010). Unattached kinetochores are sensed by the Spindle Assembly Checkpoint (SAC), which prevents anaphase onset by inhibiting the APC/C (Musacchio and Salmon, 2007). We reasoned that if activation of the SAC were responsible for the metaphase arrest, deletion of the gene encoding the central SAC component Mad2 should override the arrest. However, *mad2Δ* cells still failed to undergo a second anaphase when condensin had been released from chromosomes during the previous mitosis (Figure 1G).

An alternative pathway that blocks budding yeast cells in metaphase is the Mec1/Rad9-dependent DNA damage checkpoint (Weinert and Hartwell, 1988). Notably, deletion of the gene encoding Rad9 allowed about half of the cells that had assembled a new metaphase spindle after condensin ring cleavage to enter a second anaphase (Figures 1H-I and [Movie](#)

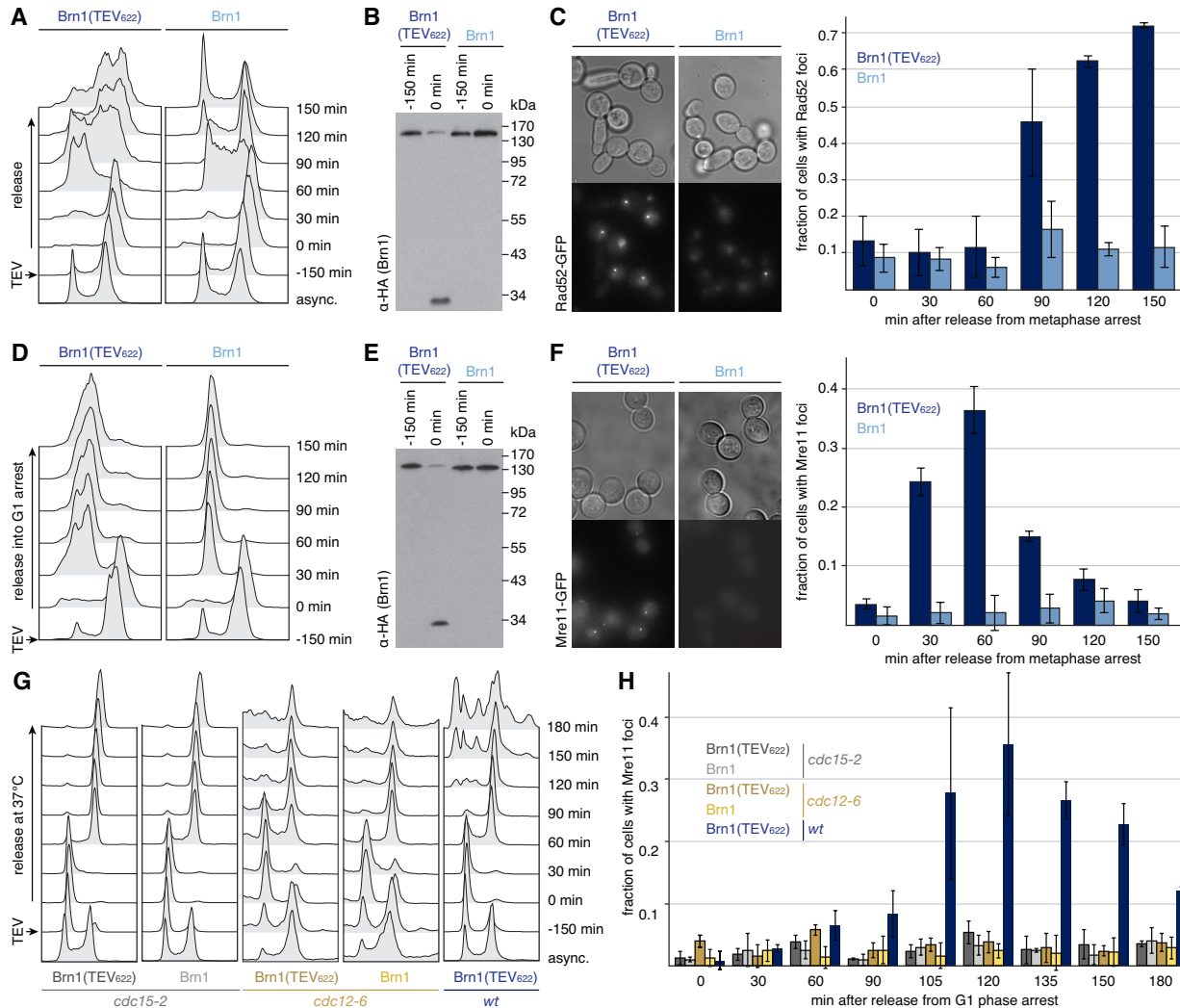
[S2](#)). Segregation of chromosomes without condensin rings attached to them might therefore result in the formation of DNA breaks, which then trigger a DNA damage checkpoint-dependent arrest in metaphase of the next cell cycle.

Chromosomes Depleted of Condensin Break During Cytokinesis

To test for the presence of DNA breaks after condensin release from chromosomes, we imaged cells that express a GFP fusion construct of the DNA double-strand break repair protein Rad52, which forms nuclear foci in response to DNA damage (Figure S1A). We cleaved condensin's Brn1 subunit in cells arrested in metaphase, released the cells from the arrest, and monitored formation of Rad52-GFP foci by fluorescence microscopy (Figures 2A-C). Strikingly, more than 70% of cells with cleaved condensin rings accumulated at least one Rad52-GFP focus within 2.5 h after the release from metaphase. In contrast,

Rad52-GFP foci were detectable in average in only 10% of cells with intact condensin rings. The fraction of cells with cleaved condensin rings that displayed Rad52-GFP foci increased notably 90 min after release from the metaphase arrest, at a time when most cells were passing through S phase (Figure 2A). DNA breaks might therefore arise during replication of chromosomes devoid of intact condensin rings. Alternatively, breaks could have occurred earlier, but might not have accumulated Rad52 until later in the cell cycle (Lisby et al., 2004).

To test whether DNA breaks form already before entry into S phase, we repeated the experiment, but this time, following condensin ring cleavage during the metaphase arrest, released cells into media containing α -factor mating pheromone to re-arrest them in G1 phase. In this case, we did not detect an increase of Rad52-GFP foci in cells with cleaved condensin rings (Figure S1B-D); most likely because Rad52 does not efficiently form foci in cells arrested in G1 phase (Figure S1E and Barlow et al., 2008). To be able to detect DNA breaks during G1 phase, we used cells that express the DNA double



strand break repair protein Mre11 fused to GFP. Notably, we detected at least one Mre11 focus in more than 35% of cells with cleaved condensin within 60 min after release into the G1 phase arrest, while Mre11-GFP foci formed in less than 5% of cells with intact condensin rings (Figure 2D-F). We conclude that DNA breaks occur before the onset of DNA replication if cells complete mitosis in the absence of chromosome-bound condensin.

Two possibilities could explain the observed chromosome breakage. First, mitotic spindle forces might rupture chromosomes that lack condensin during segregation and the breaks might somehow escape detection by the anaphase DNA damage checkpoint (Yang et al., 1997). Second, chromosome arms that fail to segregate in the absence of intact condensin and remain at the cleavage plane might be severed during cytokinesis. To distinguish between these two possibilities, we tested whether DNA breaks can be detected after anaphase chromosome segregation but before cytokinesis. Following condensin ring opening in cells arrested in G1 phase, we released cells into the cell cycle and then re-arrested them in late anaphase by inactivation of the Mitotic Exit Network (MEN) component Cdc15 (Jaspersen et al., 1998) (Figure 2G and S1F). Even though most *cdc15-2* cells had segregated their chromosome masses by 120 min after release from G1 phase (Figure S1G), we did not detect an increase in the number of cells with Mre11-GFP foci (Figure 2H). In contrast, more than 35% of *CDC15* wild-type cells with cleaved condensin rings displayed at least one Mre11-GFP focus within 120 min after release from G1 phase. Hence, exit from mitosis is required to induce DNA breakage in cells that lack condensin bound to chromosomes. Finally, we repeated the experiment in septin mutant *cdc12-6* cells (Adams and Pringle, 1984), which are unable to complete cytokinesis. Consistent with the hypothesis that DNA breaks are caused by cleavage of chromosome during cytokinesis, we observed no increase in the formation of Mre11-GFP foci in the septin mutant (Figure 2H).

Non-segregated Chromosomes Do Not Inhibit Cell Division

The finding that chromosome breaks occur only in cells that undergo cytokinesis suggests that, in the absence of chromosome-bound condensin, yeast cells divide despite the presence of non-segregated chromosomes at the cleavage plane. To directly test whether cell division proceeds, we recorded simultaneously mitotic spindle and actomyosin ring dynamics in cells expressing the α -tubulin subunit Tub1 tagged with GFP and the myosin motor subunit Myo1 tagged with mCherry after release from metaphase with intact or cleaved condensin (Figures 3A-B and Movie S3). Actomyosin contraction in cells with intact condensin commenced in average 8.6 ± 1.5 min after the onset of anaphase spindle extension (Figure 3C) and was completed after another $4.2 \text{ min} \pm 0.7$ min (Figure 3D). Timing was only marginally slower in

cells with cleaved condensin, where actomyosin ring contraction started 8.7 ± 1.7 min after anaphase onset and was completed after another 4.4 ± 1.0 min. Using the same assay, we compared the localization dynamics of chitin synthase Chs2 (Figures 3E-F and Movie S3), which is delivered to the bud neck for septum formation (Chuang and Schekman, 1996). Chs2 appeared at the bud neck 9.2 ± 1.6 min after anaphase spindle extension in cells with intact condensin and 9.5 ± 1.7 min after anaphase onset in cells with cleaved condensin (Figure 3G). Chs2 signals at the bud neck decreased as the actomyosin ring contracted and had almost completely disappeared 8.3 ± 1.5 min or 8.9 ± 1.7 min later in cells with intact or cleaved condensin rings, respectively (Figure 3H).

While the timing of cytokinetic events appears not to be considerably affected in cells that missegregate chromosomes due to condensin release, it is nevertheless conceivable that these cells might fail to physically separate. To test this possibility, we adapted a live cell microscopy assay that had been previously used in mammalian cells to probe for the completion of cytokinesis by measuring the cytoplasmic continuity between post-mitotic daughter cells (Steigemann et al., 2009). We briefly illuminated with a laser a small volume in one daughter half of dividing yeast cells expressing the GFP-variant EosFP (Wiedenmann et al., 2004) to photo-convert the emission spectrum of the EosFP molecules in this volume from green to red. If the two daughter cells were still connected, the red fluorescence signal in both daughters should rapidly equalize due to diffusion of the photo-converted EosFP (Figure 3I). In contrast, only one of the two daughters should display red fluorescence if cell division had been completed.

To validate the assay, we first photo-converted EosFP in one of the two daughter halves of cells arrested in metaphase. As expected, the red fluorescence signal rapidly diffused into the other daughter half (Figure 3J and Movie S4) and red fluorescence intensities in the two cell halves were almost equal 10 sec after photo-conversion (Figure 3K). We next released cells with cleaved or intact condensin rings (Figure S2A) from the metaphase arrest and only photo-converted EosFP in one of the two daughters after cells had entered the next cell cycle, as evident by the formation of a bud in at least one of the two daughter cells. Strikingly, diffusion of the red EosFP signal was now restricted to only the daughter cell in which EosFP had been photo-converted (Figures 3J-K and Movie S4). This experiment suggests that cells are able to complete cell division even when condensin had been released from chromosomes during the preceding metaphase. To rule out that diffusion of EosFP into the other daughter cell might merely be very slow, possibly due to the persistence of only small connections between the daughter cells, we imaged cells for 90 min after photoconversion. Still, we were not able to detect an increase in red fluorescence in the daughter cell that had not been photo-converted

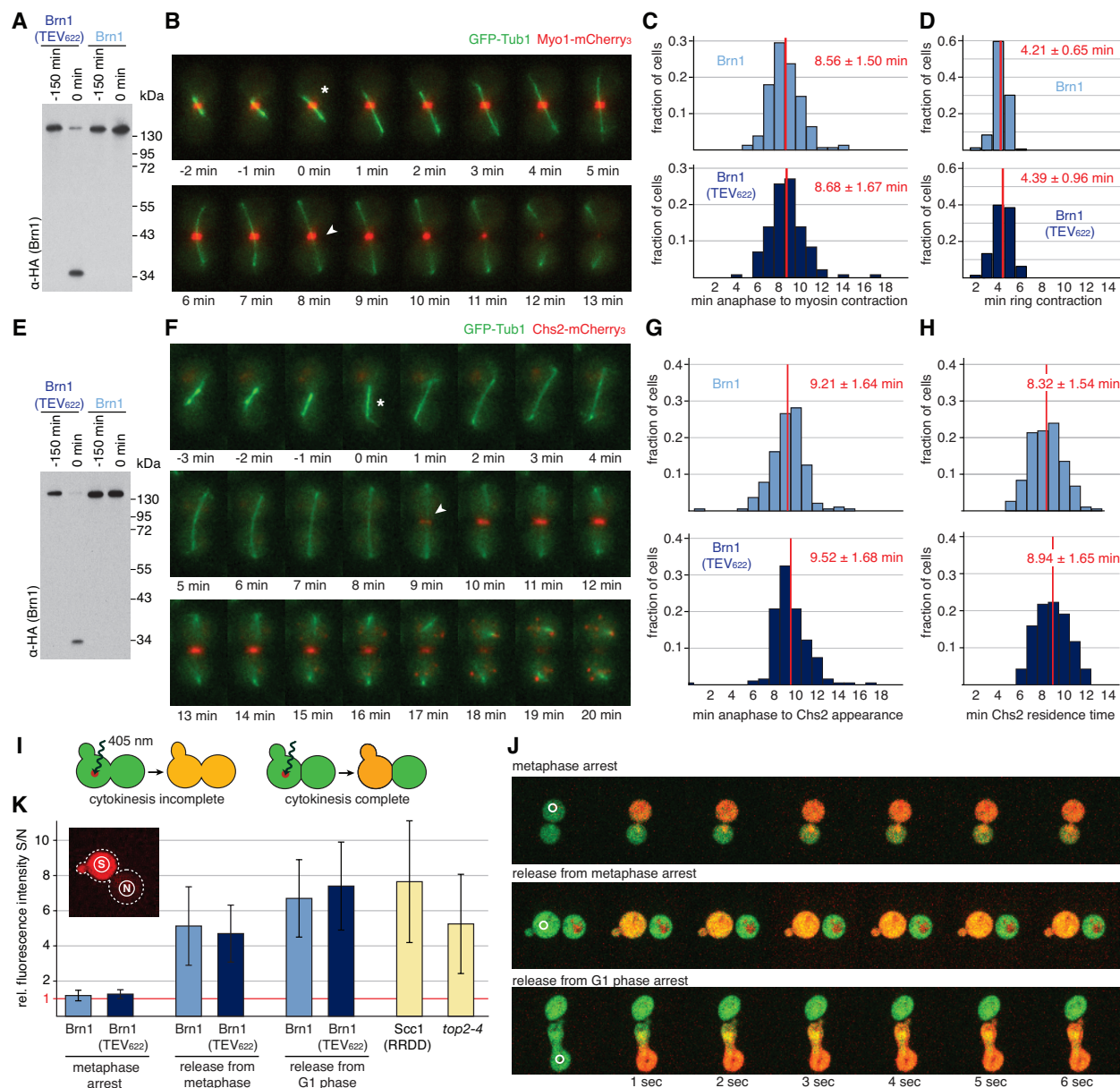


Figure 3. Cells complete division after condensin release from chromosomes

(A-D) TEV protease expression was induced in metaphase-arrested cells expressing TEV-cleavable or non-cleavable Brn1 (strains C3875 and C3898). Cells were released from the metaphase arrest by Cdc20 re-expression and actomyosin ring contraction (Myo1-mCherry₃) and mitotic spindle dynamics (GFP-Tub1) were monitored. (A) Western blotting against the C-terminal HA₆ tag on Brn1. (B) Representative image sequence of a cell expressing TEV-cleavable Brn1. Anaphase onset (asterisk) and start of actomyosin contraction (arrowhead) are indicated. Histogram plots of time (C) from anaphase onset to initiation of actomyosin ring contraction and (D) from initiation of actomyosin ring contraction to Myo1 disappearance from the bud neck ($n > 140$ cells; mean \pm SD).

(E-H) Chs2 localization dynamics (Chs2-mCherry₃) and mitotic spindle dynamics (GFP-Tub1) were monitored in cells expressing TEV-cleavable or non-cleavable Brn1 (strains C3899 and C3877) as in (A-D). (F) Anaphase onset (asterisk) and appearance of Chs2 at the bud neck (arrowhead) are indicated. Histogram plots of time (G) from anaphase onset to Chs2 appearance and (H) from Chs2 appearance and disappearance at the bud neck ($n > 180$ cells; mean \pm SD).

(I-K) EosFP was photoconverted from green to red fluorescence in a small area in one daughter half of cells expressing non-cleavable or TEV-cleavable Brn1. (I) Diffusion of photoconverted EosFP would rapidly equalize the fluorescence spectra of both daughters if they were still connected (left) but not if cytokinesis had been completed (right). (J) Image sequences after photo-conversion of EosFP (white circles) after Brn1 TEV cleavage in cells arrested in metaphase (top) or released from the metaphase arrest (middle, strain C3099) or in cells released from G1 phase (bottom, strain C3246). (K) Red fluorescence excitation intensities in photo-converted (switched, S) and non-converted (non-switched, N) daughter cells were measured 10 sec (metaphase arrest and release; strains C3099 and C3100) or 30 sec (G1 phase release; strains C3246 and C3233) after photoconversion. In addition, fluorescence intensity ratios were measured of cells released from a G1 phase arrest after overexpression of a non-cleavable version of Scc1 (strain C3144) or of top2-4 mutant cells (strain C3145) released from a metaphase arrest at the restrictive temperature. Mean intensity ratios (S/N) \pm SD are shown ($n = 21-45$ cells).

See also [Figure S2](#) and [Movies S3](#) and [S4](#).

(Figure S2B). Finally, we cleaved condensin already during G1 phase, released cells into the cell cycle and then photo-converted EosFP at the distal end of the elongated daughter cell once cells had formed a new bud. While we were able to follow the rapid diffusion of photo-converted EosFP along the axis of the cell, we could not detect an increase in red fluorescence in the other daughter (Figures 3J-K and Movie S4). We conclude that the chromosome segregation failures that result from condensin release from chromosomes do not prevent the completion of cell division.

It has been suggested that the presence of non-segregated chromosomes at the plane of cell division is sensed by the 'NoCut' checkpoint pathway, which delays completion of cytokinesis in order to prevent chromosome breakage (Mendoza et al., 2009; Norden et al., 2006). The finding that cells divide after condensin cleavage despite the presence of lagging chromosomes raises the possibility that condensin might be part of a pathway that links chromosome segregation to cytokinesis (Bembenek et al., 2013). We therefore tested whether cell division measured by our assay is inhibited when we prevent chromosome segregation in the presence of intact condensin. First, we over-expressed in cells arrested in G1 phase a version of the cohesin subunit Scc1 that cannot be cleaved by separase (Figure S2C). When released from the G1 arrest, cells fail to resolve cohesion and attempt cell division without sister chromatid separation (Uhlmann et al., 1999). In these cells, we could still not detect diffusion of EosFP from one daughter cell into the other (Figure 3K), despite severe chromosome segregation failures (Figure S2C). Second, we inhibited sister chromatid resolution by inactivation of topo II, which causes the bulk of chromatin to span across the bud neck (Figure S2D). Again, we did not detect diffusion of EosFP between the daughter cells (Figure 3K). In summary, our results demonstrate that cell division can proceed to a level that prevents diffusion of a small protein (~28 kDa) even when non-segregated chromosomes are present at the cleavage plane, independent of whether condensin is bound to these chromosomes or not.

Condensin Ring Integrity is Sufficient to Allow Chromosome Arm Segregation

Our experiments suggest that the failure to segregate chromosomes during anaphase results from the release of condensin from chromosomes by ring opening. We wondered whether restoring the ring integrity of cleaved condensin complexes at the metaphase-to-anaphase transition might then be sufficient to restore condensin function. We engineered into Brn1 TEV sites flanked by two repeats of the human FKBP12 and Frb proteins, which, in the presence of the small molecule rapamycin, form stable heterodimers (Gruber et al., 2006). Addition of rapamycin after condensin ring opening by TEV

cleavage should therefore allow condensin ring re-closure (Figure 4A).

We first tested whether rapamycin-induced dimerization is sufficiently strong to maintain the function of condensin rings after Brn1 cleavage. We induced TEV protease expression in asynchronous cells that express Brn1 with FKBP12- and Frb-flanked TEV sites inserted into one of two different positions and plated cells onto media with or without rapamycin. While these cells failed to grow in the absence of rapamycin, they proliferated indistinguishable from cells that express non-cleavable Brn1 in the presence of rapamycin (Figure 4B). Keeping condensin rings closed by FKBP12-Frb-mediated dimerization is hence sufficient to maintain condensin function.

We next tested whether ring re-closure at different cell cycle stages could restore condensin function. First, we cleaved Brn1 in cells arrested in G1 phase and then plated them immediately (Figure S3A) or after allowing them to progress into a nocodazole-induced mitotic arrest (Figure S3B) onto media with or without rapamycin. In both cases, cells grew comparable to cells with intact condensin on media with rapamycin but failed to grow on media without rapamycin. To assay whether re-closure of condensin rings rescues chromosome segregation defects, we cleaved Brn1 in cells arrested in G1 phase (Figure S3C), then released cells from the arrest into media with or without rapamycin and monitored segregation of a fluorescent marker array integrated at the distal end of the long arm of chromosome V by time-lapse microscopy (Figure 4C and D). In the absence of rapamycin, only 26% of cells with cleaved condensin rings successfully segregated the labeled chromosome arm into the two daughter cells within 165 min after release from the G1 phase arrest. Addition of rapamycin by the time of release increased the fraction of cells with successfully segregated chromosome V arms to 61% (Figure 4D). Rapamycin had no notable effect on chromosome segregation in cells with intact condensin rings, which achieved a maximum of 76% segregation within the duration of the time course (Figure S3C-E). We conclude that condensin ring re-closure after exit from G1 phase is able to rescue chromosome arm segregation to a considerable degree.

Finally, we asked whether condensin ring re-closure at the transition from metaphase to anaphase would be sufficient to prevent chromosome arm missegregation. We cleaved condensin in metaphase-arrested cells (Figure S3F), then released the cells from the arrest and scored segregation of chromosome arm V (Figure 4E and F). Without addition of rapamycin, only 35% of cells segregated the labeled chromosome arm equally between the daughter cells. When we added rapamycin shortly before releasing cells into anaphase, the fraction of cells that correctly segregated chromosome arm V increased to 58% (Figure 4F). For comparison, up to 76% of cells with intact condensin rings segregated chromosome arm V equally in this experiment, independent of whether we had

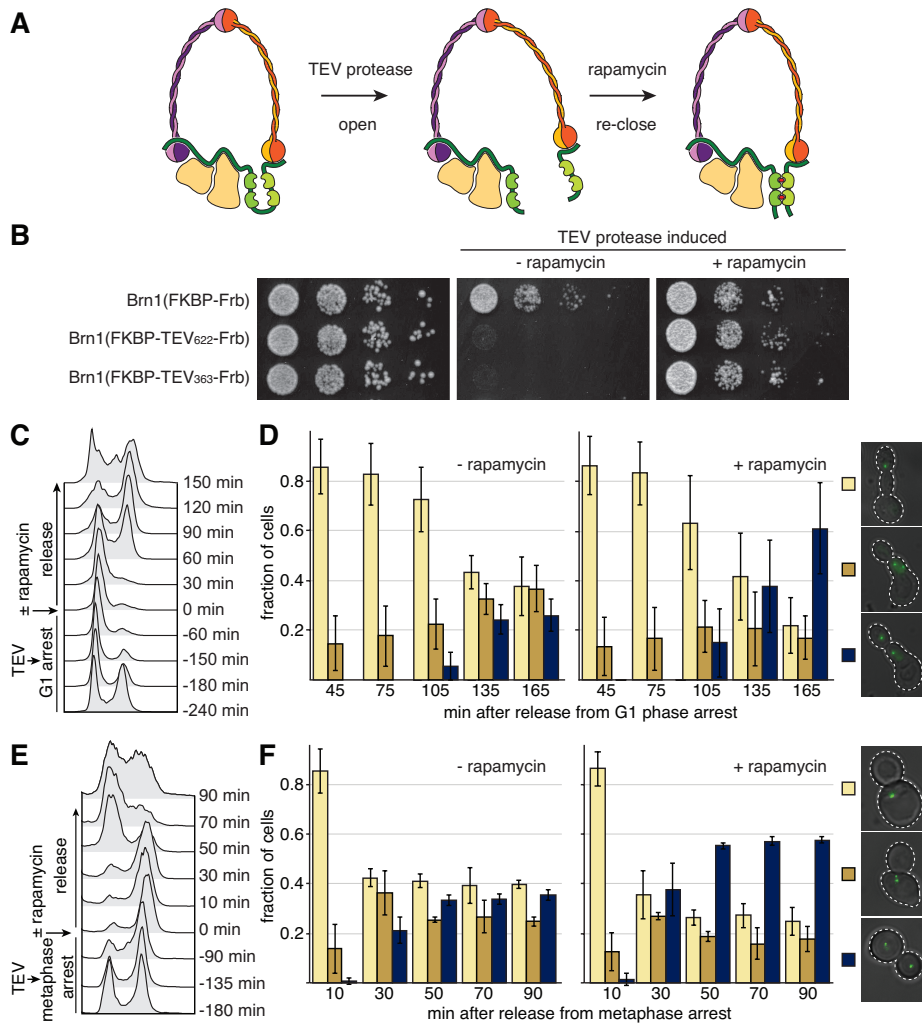


Figure 4. Condensin ring re-closure restores chromosome arm segregation

(A) Condensin rings were opened by site-specific cleavage of Brn1 at TEV protease target sites flanked by two FKBP and Frb domains. Addition of rapamycin induces FKBP and Frb dimerization and thereby closes the ring structure.

(B) TEV protease expression was induced in asynchronously growing cultures (strains C3671, C3574, and C3572) before plating cells on media with or without rapamycin.

(C-D) TEV protease expression was induced in G1 phase-arrested cells expressing Brn1(FKBP₂-TEV₆₂₂-Frb₂) (strain C3574) before release into media with or without rapamycin. (C) Cell cycle progression was monitored by FACS analysis of cellular DNA content (-rapamycin culture). (D) Segregation of a GFP marker array integrated proximal to the right telomere of chromosome V was scored by live cell microscopy. Data represent the mean of quadruplicate experiments \pm SD from 20-39 cells per experiment.

(E-F) TEV protease expression was induced in metaphase-arrested cells expressing Brn1(FKBP₂-TEV₆₂₂-Frb₂) (strain C3629) before release into media with or without rapamycin. Cell cycle progression and chromosome V segregation were scored as in (C-D). Data represent the mean of triplicate experiments \pm SD from 39-84 cells per experiment.

See also Figure S3.

added rapamycin or not (Figure S3F-H). Re-closure of cleaved condensin rings shortly before anaphase onset is hence sufficient to restore the correct segregation of long chromosome arms in a substantial fraction of cells.

DISCUSSION

The nature and consequences of the segregation failures that are hallmarks of cells devoid of condensin function have remained poorly understood. Our live cell imaging experiments suggest that, following condensin release from chromosomes by opening its ring structure, cells proceed through and exit from mitosis with similar timing as cells with intact condensin (Figure 3A-H). However, upon completion of cytokinesis, cells with cleaved condensin accumulate chromosome breaks (Figure 2) and consequently arrest in a DNA damage checkpoint-dependent manner (Figure 1). These findings suggest that trailing chromosome arms, which fail to clear the cytokinetic cleavage plane when condensin is not bound to them, are severed either by the forces generated by the

contracting cleavage furrow or during abscission. We hypothesize that condensin's primary function might therefore be to tighten chromosome arms, potentially by creating topological linkages (Cuyley et al., 2011), in order to ensure that the arms are moved all the way to the cell poles during anaphase. Remarkably, restoring condensin topology just before anaphase onset is sufficient to allow proper chromosome arm segregation in a considerable fraction of cells (Figure 4F). If condensin acts as an intra-chromosomal linker molecule, then it must be possible that functional links form *de novo* at the time of metaphase.

The discovery that non-segregated chromosomes are broken during cytokinesis is surprising, since we expect that chromatin trapped in the cleavage furrow should be detected by the NoCut pathway, which was suggested to delay abscission and thereby allow completion of segregation and prevent chromosome breakage (Mendoza et al., 2009; Norden et al., 2006). While cytokinesis and entry into the next cell cycle might be minimally delayed in cells with cleaved condensin rings (Figures 1D and 3A-H), any such delay would obviously be insufficient to prevent

chromosome breakage. Our findings are consistent with the formation of DNA breaks in yeast cells that are prevented from completing chromosome segregation by topo II depletion (Baxter and Diffley, 2008) or from resolving sister rDNA loci after Cdc14 inactivation/re-activation (Quevedo et al., 2012). Since the latter results in a delay in karyokinesis, it might have been conceivable that chromosome-bound condensin is required for activation of the NoCut pathway. However, our finding that cells complete cytokinesis irrespective of whether chromosome segregation had been prevented due to condensin cleavage, a failure to resolve cohesion, or topo II inactivation (Figure 3K) argues against this hypothesis.

Even though cytokinesis-induced DNA breaks are detected already during G1 phase (Figure 2F), cells proceed through S phase and only arrest in the next metaphase; similar to cells that fail to disjoin chromosome XII (Quevedo et al., 2012). Why do these breaks not trigger a G1/S or intra-S phase DNA damage checkpoint (Longhese et al., 1998)? One possibility is that only very few chromosome arms might get severed during cytokinesis, which could be insufficient to set off a pathway response before G2/M (Zierhut and Diffley, 2008). This is consistent with the finding that the gross of chromosomes in condensin mutants appears intact in pulsed-field gel electrophoresis analyses (Lavoie et al., 2002). A second possibility is that the type of DNA breaks generated might not be capable of eliciting G1 or S phase checkpoints (Barlow et al., 2008). Alternatively, processing by the non-homologous end joining (NHEJ) repair machinery might mask the DNA breaks. The latter possibility is, however, unlikely, since cells with cleaved condensin that lack the NHEJ component Ku70 still arrest only in metaphase (Figure 1J). The only possibility to rescue the broken chromosome ends might therefore be either *de novo* telomere addition (Kramer and Haber, 1993) or fusion to other chromosomes, with the latter entailing the danger to create breakage-fusion-bridge cycles (McClintock, 1939) that could lead to chromosome structure aberrations similar to those recently described in human cells (Gascoigne and Cheeseman, 2013; Janssen et al., 2011). Strikingly, formation of DNA breaks has also been observed in human cells depleted for the condensin subunit Smc2 (Samoshkin et al., 2012). Condensin's function in preventing damage to trailing chromosome arms might therefore be conserved from yeast to humans.

EXPERIMENTAL PROCEDURES

Yeast strains. All strains are derivatives of W303; detailed genotypes and culture conditions are listed in the supplemental information.

Live cell microscopy. Cells were transferred onto glass-bottom dishes (MatTek) coated with concanavalin A (Sigma), allowed to settle for 10 min, and then washed three times with – MET or synthetic complete medium (SC) containing 2%

raffinose and 2% galactose. Cells were then covered with the same medium and imaged at the indicated time points at 30°C or 37°C (Figure 2H). To monitor the formation of DNA breaks (Rad52-GFP or Mre11-GFP), a fresh batch of cells was transferred to a new dish for each time point to avoid photo-induced DNA damage. To monitor in parallel segregation of chromosome V in the presence and absence of rapamycin, multi-well microscopy slides (ibidi) were used.

Imaging was performed on a DeltaVision Spectris Restoration microscope (Applied Precision) with a 100×, NA 1.35 oil immersion objective. To monitor spindle formation, 12 z-sections with 700 nm step size and 0.07 s exposure times at 50% transmission of the GFP filter were recorded every 3 min. To reduce light exposure of the *rad9Δ* strain, 16 z-sections with 300 nm step size and 0.07 s exposure times at 32% transmission of the GFP filter were recorded only every 10 min. Rad52-GFP and Mre11-GFP foci were recorded at 12 z-sections and chromosome V GFP arrays were recorded at 15 z-sections with 700 nm step size and 0.2 s exposure times at 100% transmission of the GFP filter. To monitor cytokinesis dynamics, GFP and mCherry images were captured with 6 z-sections of 1 μm step size every minute using 2×2 binning. Exposure times were 0.05 s at 32% transmission for GFP and 0.1 s at 50% transmission for mCherry.

Photoconversion experiments. Cytoplasmic EosFP in a circular spot with 2.1 μm diameter was photo-converted in one daughter cell by three 10 msec pulses from a 405 nm laser set to 1% intensity on an UltraVIEW VoX spinning disk microscope (Perkin-Elmer). Transmission, red, and green fluorescence images were recorded every second from 1 s before to 30 s after conversion at 50 msec exposure and 5% laser power. To quantify the diffusion between daughter cells, the mean fluorescence signals of the red channel were measured in a circular area of 3.3 μm diameter in the photo-switched cell (S) and the non-converted cell (N) and the S/N ratio calculated after background subtraction

SUPPLEMENTAL INFORMATION

Supplemental Information includes Figures S1-S3, Movies S1-S4, and Supplemental Experimental Procedures, and can be found with this article online.

ACKNOWLEDGEMENTS

We are grateful to S. Gruber, M. Knop, D. Liakopoulos, M. Meurer, K. Nasmyth, and S. Piatti for providing plasmids and strains and to the EMBL Advanced Light Microscopy Facility (ALMF) and the Flow Cytometry Core Facility for assistance. We thank Perkin-Elmer for continued support of the ALMF. This work was supported by funding from EMBL and the German Research Foundation (DFG Priority Programme 1384).

REFERENCES

- Adams, A.E., and Pringle, J.R. (1984). Relationship of actin and tubulin distribution to bud growth in wild-type and morphogenetic-mutant *Saccharomyces cerevisiae*. *J Cell Biol* **98**, 934–945.
- Barlow, J.H., Lisby, M., and Rothstein, R. (2008). Differential regulation of the cellular response to DNA double-strand breaks in G1. *Mol Cell* **30**, 73–85.
- Baxter, J., Sen, N., Martínez, V.L., De Carandini, M.E.M., Schwartzman, J.B., Diffley, J.F.X., and Aragón, L. (2011). Positive supercoiling of mitotic DNA drives decatenation by topoisomerase II in eukaryotes. *Science* **331**, 1328–1332.
- Baxter, J., and Diffley, J.F.X. (2008). Topoisomerase II inactivation prevents the completion of DNA replication in budding yeast. *Mol Cell* **30**, 790–802.
- Bembenek, J.N., Verbrugghe, K.J.C., Khanikar, J., Csankovszki, G., and Chan, R.C. (2013). Condensin and the Spindle Midzone Prevent Cytokinesis Failure Induced by Chromatin Bridges in *C. elegans* Embryos. *Curr Biol* **23**, 937–946.
- Brito, I.L., Yu, H.-G., and Amon, A. (2010). Condensins promote coorientation of sister chromatids during meiosis I in budding yeast. *Genetics* **185**, 55–64.
- Carlton, J.G., Caballe, A., Agromayor, M., Kloc, M., and Martin-Serrano, J. (2012). ESCRT-III governs the Aurora B-mediated abscission checkpoint through CHMP4C. *Science* **336**, 220–225.
- Chuang, J.S., and Schekman, R.W. (1996). Differential trafficking and timed localization of two chitin synthase proteins, Chs2p and Chs3p. *J Cell Biol* **135**, 597–610.
- Cuylen, S., and Haering, C.H. (2011). Deciphering condensin action during chromosome segregation. *Trends Cell Biol* **21**, 552–559.
- Cuylen, S., Metz, J., and Haering, C.H. (2011). Condensin structures chromosomal DNA through topological links. *Nat Struct Mol Biol* **18**, 894–901.
- D'Ambrosio, C., Kelly, G., Shirahige, K., and Uhlmann, F. (2008). Condensin-dependent rDNA decatenation introduces a temporal pattern to chromosome segregation. *Curr Biol* **18**, 1084–1089.
- D'Amours, D., Stegmeier, F., and Amon, A. (2004). Cdc14 and condensin control the dissolution of cohesin-independent chromosome linkages at repeated DNA. *Cell* **117**, 455–469.
- Fujiwara, T., Bandi, M., Nitta, M., Ivanova, E.V., Bronson, R.T., and Pellman, D. (2005). Cytokinesis failure generating tetraploids promotes tumorigenesis in p53-null cells. *Nature* **437**, 1043–1047.
- Gascoigne, K.E., and Cheeseman, I.M. (2013). Induced dicentric chromosome formation promotes genomic rearrangements and tumorigenesis. *Chromosome Res* **21**, 407–418.
- Gruber, S., Arumugam, P., Katou, Y., Kuglitsch, D., Helmhart, W., Shirahige, K., and Nasmyth, K. (2006). Evidence that loading of cohesin onto chromosomes involves opening of its SMC hinge. *Cell* **127**, 523–537.
- Hirano, T., Funahashi, S., Uemura, T., and Yanagida, M. (1986). Isolation and characterization of *Schizosaccharomyces pombe* cutmutants that block nuclear division but not cytokinesis. *Embo J* **5**, 2973–2979.
- Hirano, T. (2012). Condensins: universal organizers of chromosomes with diverse functions. *Genes Dev* **26**, 1659–1678.
- Janssen, A., van der Burg, M., Szuhai, K., Kops, G.J.P.L., and Medema, R.H. (2011). Chromosome segregation errors as a cause of DNA damage and structural chromosome aberrations. *Science* **333**, 1895–1898.
- Jaspersen, S.L., Charles, J.F., Tinker-Kulberg, R.L., and Morgan, D.O. (1998). A late mitotic regulatory network controlling cyclin destruction in *Saccharomyces cerevisiae*. *Mol Biol Cell* **9**, 2803–2817.
- Kramer, K.M., and Haber, J.E. (1993). New telomeres in yeast are initiated with a highly selected subset of TG1-3 repeats. *Genes Dev* **7**, 2345–2356.
- Lavoie, B.D., Hogan, E., and Koshland, D. (2002). In vivo dissection of the chromosome condensation machinery: reversibility of condensation distinguishes contributions of condensin and cohesin. *J Cell Biol* **156**, 805–815.
- Lisby, M., Barlow, J.H., Burgess, R.C., and Rothstein, R. (2004). Choreography of the DNA damage response: spatiotemporal relationships among checkpoint and repair proteins. *Cell* **118**, 699–713.
- Longhese, M.P., Foiani, M., Muzi-Falconi, M., Lucchini, G., and Plevani, P. (1998). DNA damage checkpoint in budding yeast. *Embo J* **17**, 5525–5528.
- McClintock, B. (1939). The Behavior in Successive Nuclear Divisions of a Chromosome Broken at Meiosis. *Proc Natl Acad Sci USA* **25**, 405–416.
- McGrew, J.T., Goetsch, L., Byers, B., and Baum, P. (1992). Requirement for ESP1 in the nuclear division of *Saccharomyces cerevisiae*. *Mol Biol Cell* **3**, 1443–1454.
- Mendoza, M., Norden, C., Durrer, K., Rauter, H., Uhlmann, F., and Barral, Y. (2009). A mechanism for chromosome segregation sensing by the NoCut checkpoint. *Nat Cell Biol* **11**, 477–483.
- Mullins, J.M., and Biesele, J.J. (1977). Terminal phase of cytokinesis in D-98s cells. *J Cell Biol* **73**, 672–684.
- Musacchio, A., and Salmon, E.D. (2007). The spindle-assembly checkpoint in space and time. *Nat Rev Mol Cell Biol* **8**, 379–393.
- Norden, C., Mendoza, M., Dobbelaere, J., Kotwaliwale, C.V., Biggins, S., and Barral, Y. (2006). The NoCut pathway links completion of cytokinesis to spindle midzone function to prevent chromosome breakage. *Cell* **125**, 85–98.
- Piazza, I., Haering, C.H., and Rutkowska, A. (2013). Condensin: crafting the chromosome landscape. *Chromosoma* **22**, 175–90.
- Quevedo, O., García-Luis, J., Matos-Perdomo, E., Aragón, L., and Machin, F. (2012). Nondisjunction of a single chromosome leads to breakage and activation of DNA damage checkpoint in g2. *PLoS Genet* **8**, e1002509.
- Renshaw, M.J., Ward, J.J., Kanemaki, M., Natsume, K., Nédélec, F.J., and Tanaka, T.U. (2010). Condensins promote chromosome recoiling during early anaphase to complete sister chromatid separation. *Dev Cell* **19**, 232–244.
- Samoshkin, A., Dulev, S., Loukinov, D., Rosenfeld, J.A., and Strunnikov, A.V. (2012). Condensin dysfunction in human cells induces nonrandom chromosomal breaks in anaphase, with distinct patterns for both unique and repeated genomic regions. *Chromosoma* **121**, 191–199.
- Shi, Q., and King, R.W. (2005). Chromosome nondisjunction yields tetraploid rather than aneuploid cells in human cell lines. *Nature* **437**, 1038–1042.
- Steigemann, P., Wurzenberger, C., Schmitz, M.H.A., Held, M., Guizetti, J., Maar, S., and Gerlich, D.W. (2009). Aurora B-mediated abscission checkpoint protects against tetraploidization. *Cell* **136**, 473–484.
- Uhlmann, F., Lottspeich, F., and Nasmyth, K. (1999). Sister-chromatid separation at anaphase onset is promoted by cleavage of the cohesin subunit Scc1. *Nature* **400**, 37–42.
- Weinert, T.A., and Hartwell, L.H. (1988). The RAD9 gene controls the cell cycle response to DNA damage in *Saccharomyces cerevisiae*. *Science* **241**, 317–322.
- Wiedenmann, J., Ivanchenko, S., Oswald, F., Schmitt, F., Röcker, C., Salih, A., Spindler, K.-D., and Nienhaus, G.U. (2004). EosFP, a fluorescent marker protein with UV-inducible green-to-red fluorescence conversion. *Proc Natl Acad Sci USA* **101**, 15905–15910.
- Yang, S.S., Yeh, E., Salmon, E.D., and Bloom, K. (1997). Identification of a mid-anaphase checkpoint in budding yeast. *J Cell Biol* **136**, 345–354.
- Zierhut, C., and Diffley, J.F.X. (2008). Break dosage, cell cycle stage and DNA replication influence DNA double strand break response. *Embo J* **27**, 1875–1885.

SUPPLEMENTAL INFORMATION

SUPPLEMENTAL FIGURES

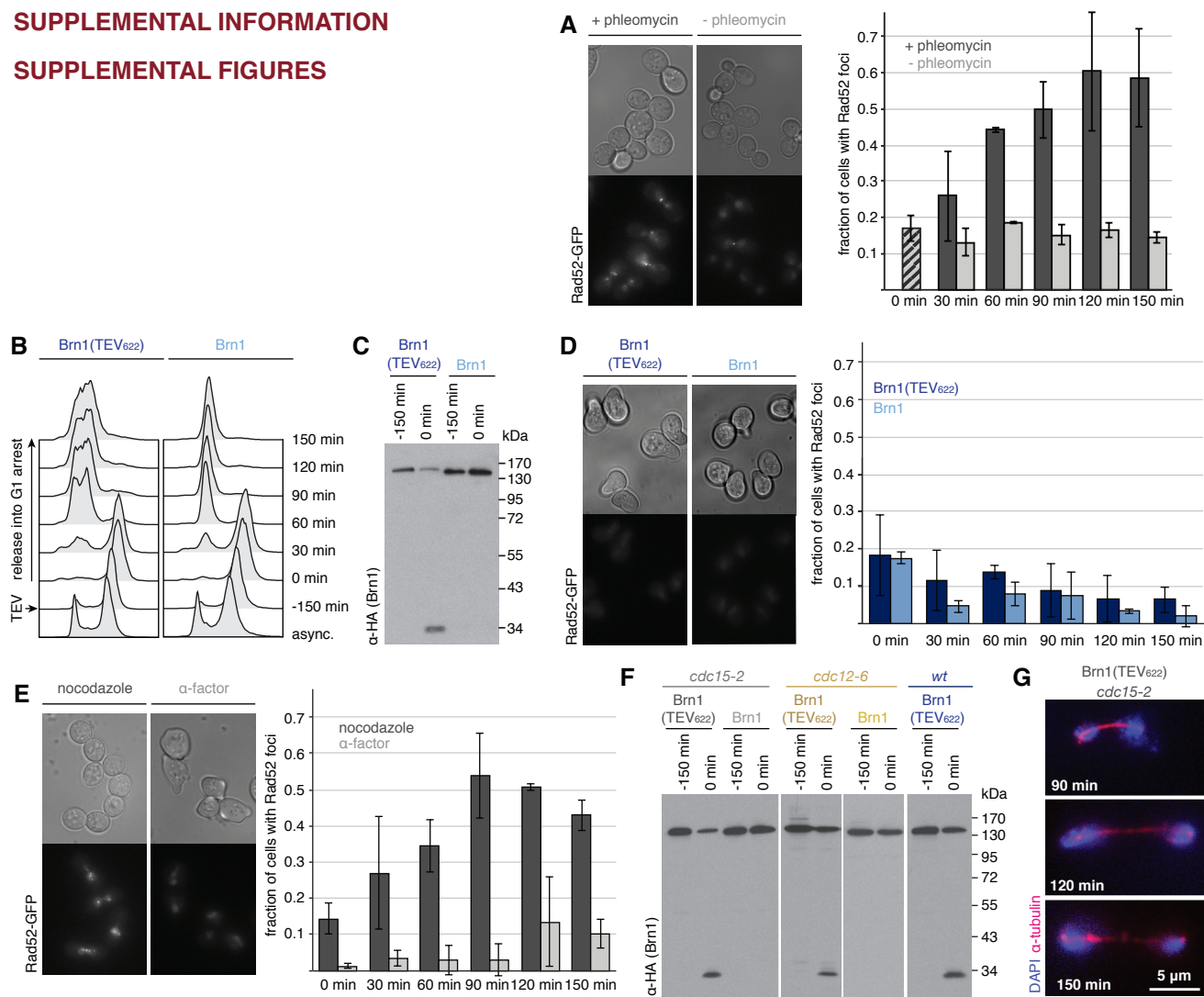


Figure S1. DNA double-strand break formation after condensin release from chromosomes (related to Figure 2)

(A) Asynchronous cultures of cells expressing Rad52-GFP (strain C3294) were incubated with and without 10 μ g/ml phleomycin and the fraction of cells with at least one Rad52-GFP focus was scored every 30 min after phleomycin addition. Example images from the 120 min time point are shown.

(B-D) TEV protease expression was induced in cells expressing Rad52-GFP and TEV-cleavable or non-cleavable Brn1 (strains C3310 and C3308) arrested in metaphase by Cdc20 depletion. Cells were released from the arrest after TEV induction. (B) Cell cycle progression was monitored by FACScan analysis of cellular DNA content. (C) Brn1 cleavage was monitored by western blotting against the HA₆ epitope tag fused to the C terminus of Brn1. (D) The fraction of cells with at least one Rad52-GFP focus was scored every 30 min after release. Example images from the 150 min time point are shown.

(E) Cells expressing Rad52-GFP (strain C3294) were arrested either in G1 phase by α -factor or in mitosis by addition of nocodazole and the fraction of cells with at least one Rad52-GFP focus was scored every 30 min after addition of phleomycin to 10 μ g/ml. Example images from the 120 min time point are shown.

(F) Western blot against the C-terminal HA₆ epitope tag on Brn1 before and after TEV protease induction in cells arrested in G1 phase at 25°C (strains C3432, C3434, C3801, C3796, and C3381).

(G) Anaphase arrest of *cdc15-2* cells (strain C3432) was confirmed by co-staining fixed cells at the indicated time points after release from the G1 phase arrest for mitotic spindles with α -tubulin antibody and for DNA with DAPI.

In (A, D and E), data represent the mean of duplicate experiments \pm SD (n = 28-70 cells per time point and experiment).

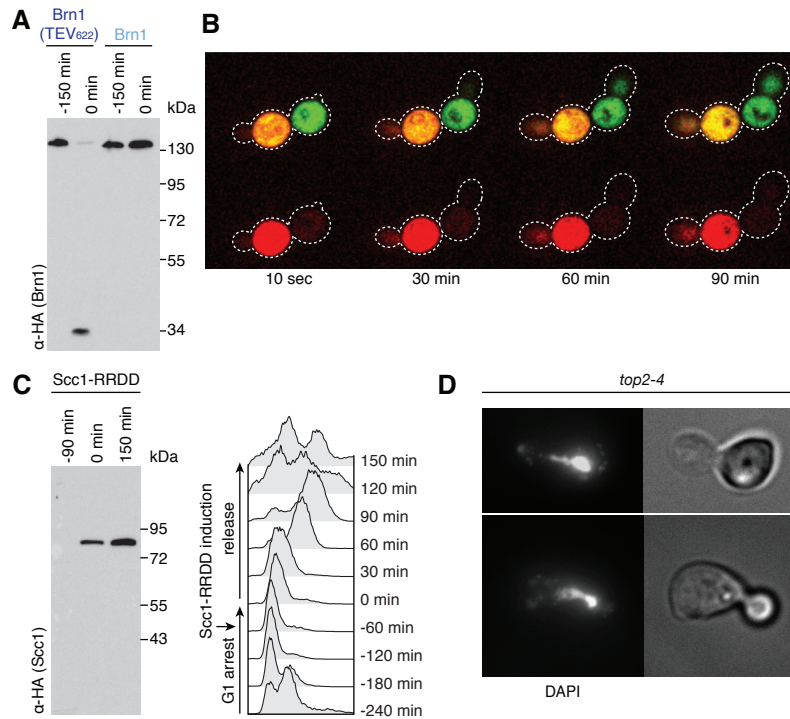


Figure S2. Cytokinesis proceeds despite segregation failures (related to Figure 3)

(A) Western blot against the C-terminal HA₃ epitope tag on Brn1 before and after TEV protease induction in metaphase-arrested cells expressing TEV-cleavable or non-cleavable Brn1 and EosFP (strains C3099 and C3100).

(B) TEV cleavage of Brn1 was induced in cells (strain C3099) arrested in metaphase by Cdc20 depletion. Cells were then released from the arrest, photoconversion of Eos was triggered 80 min after the release in one of two daughter cells after bud formation, and images were taken immediately after photoconversion and then every 30 min for 1.5 h.

(C) Cells (strain C3144) were arrested in G1 phase with α-factor. Expression of non-cleavable Scc1 was induced by galactose addition and monitored by western blotting against the HA₃ tag fused to the C terminus of Scc1-RRDD. Cells were then released from the G1 phase arrest and cell cycle progression was monitored by FACScan analysis of cellular DNA content.

(D) *top2-4* mutant cells (strain C3145) were arrested in G1 phase with α-factor and then released from the arrest at 37°C. Two hours after release, cells were fixed and DNA was stained with DAPI.

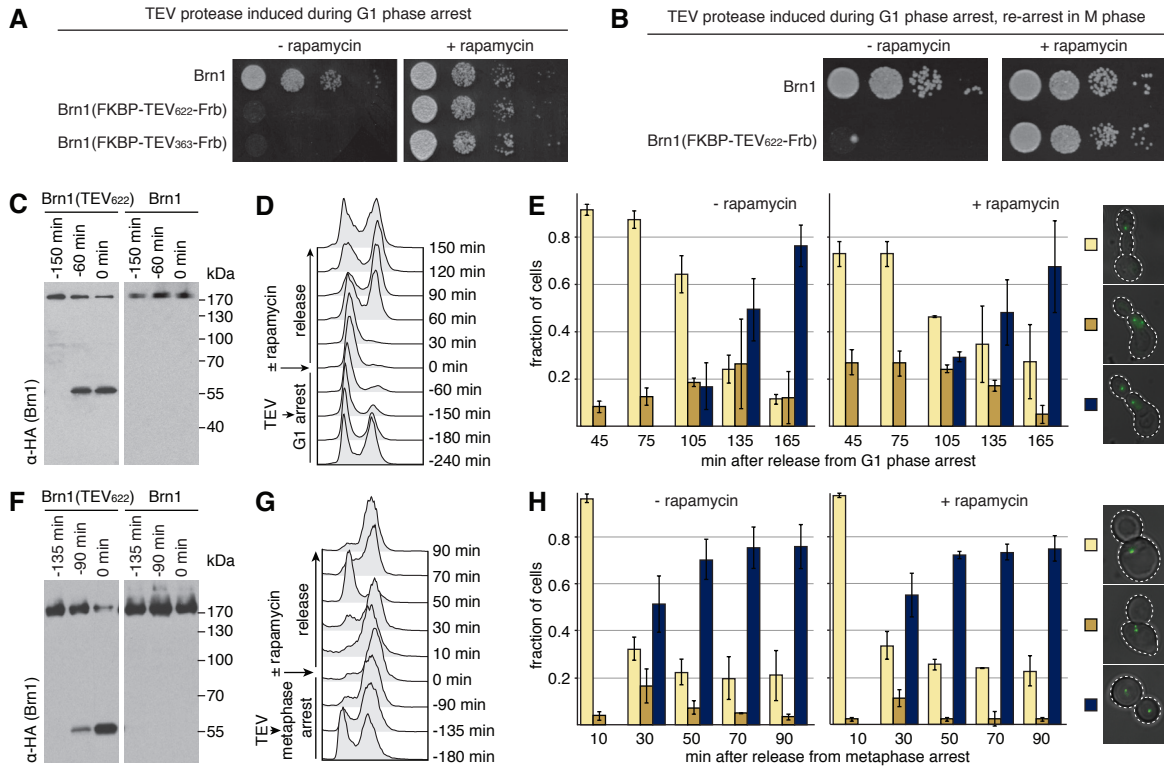


Figure S3. Ring re-closure restores condensin function (related to [Figure 4](#))

(A) TEV protease expression was induced by galactose addition for 2.5 h in cells (strains C3671, C3574, and C3572) arrested in G1 phase with α -factor before plating cells on galactose plates with or without rapamycin.

(B) TEV protease expression was induced by galactose addition for 2.5 h in cells (strains C3372, C3378) arrested in G1 phase with α -factor and cells were released into medium containing nocodazole to re-arrest them in mitosis. Cells were filtered after 1.5 h and released on galactose plates with or without rapamycin.

(C-E) TEV protease expression was induced for 2.5 h in cells arrested in G1 phase. Cells were then released from the arrest. (C) Brn1 cleavage was monitored by immunoblotting against the C-terminal HA₆ tag fused to Brn1 at the indicated time points before release from the arrest (strains C3574 and C3671). (D) Cell cycle progression was monitored by FACScan analysis of cellular DNA content of cells expressing non-cleavable Brn1 (strain C3671). (E) Segregation of telV markers in cells expressing non-cleavable Brn1 (strain C3671) were scored at the indicated time points. Data represent the mean of duplicate experiments \pm SD ($n = 10$ -46 cells per experiment).

(F-H) TEV protease expression was induced for 2.25 h in cells arrested in metaphase. Cells were then released from the arrest. (F) Brn1 cleavage was monitored as in (C) (strains C3629 and C3696). (G) Cell cycle progression of cells expressing non-cleavable Brn1 (strain 3696) was monitored as in (D). (H) TelV marker segregation in cells expressing non-cleavable Brn1 (strain 3696) was scored at the indicated time points as in (E). Data represent the mean of duplicate experiments \pm SD ($n = 42$ -97 cells per experiment).

SUPPLEMENTAL MOVIES

Movie S1. Mitotic spindle dynamics in cells with intact or cleaved Brn1 (related to [Figure 1](#))

Time-lapse recording of cells expressing GFP-Tub1 and a non-cleavable (top; strain C3257) or TEV-cleavable (bottom; strain C3258) version of Brn1. Time is indicated in hours and minutes after release from the metaphase arrest.

Movie S2. Mitotic spindle dynamics in a *rad9Δ* cell with cleaved Brn1 (related to [Figure 1](#))

Time-lapse recording of a *rad9Δ* cell expressing TEV-cleavable Brn1 and GFP-Tub1 (strain C3512). Time is indicated in hours and minutes after release from the metaphase arrest.

Movie S3. Mitotic spindle, actomyosin ring, and Chs2 localization dynamics in cells with cleaved Brn1 (related to [Figure 3](#))

Time-lapse recording of cells that express GFP-Tub1 (green) and Myo1-mCherry₃ (red) (left; strain C3875) or GFP-Tub1 (green) and Chs2-mCherry₃ (red) (right; strain C3899) after release from metaphase. Time is indicated relative to anaphase onset.

Movie S4. EosFP diffusion in cells with cleaved Brn1 (related to [Figure 3](#))

Time-lapse recording of EosFP-expressing cells after Brn1 cleavage during the metaphase arrest (left; strain C3099), after Brn1 cleavage and release from the metaphase arrest (middle; strain C3099), or after Brn1 cleavage and release from G1 phase (right; strain C3246). EosFP was photoconverted in one daughter cell and distribution of red and green fluorescence signals recorded. Time is indicated relative to photo-conversion.

SUPPLEMENTAL EXPERIMENTAL PROCEDURES

Yeast cell culture and synchronization. For arrest in G1 phase, cells were grown at 25°C ([Figure 2G-H](#)) or 30°C (all other experiments) in yeast extract peptone containing 2% raffinose (YEP-R) to mid-log phase, collected by filtration, washed with dH₂O, and resuspended at an OD₆₀₀ of 0.15 in YEP-R containing 3 μg/ml α-factor. After 1 h, additional α-factor was added to 2 μg/ml and 30 min later galactose was added to 2% to induce TEV protease induction. After another 30 min, cells were collected by filtration, washed with dH₂O, and resuspended in fresh YEP-R with 2% galactose (YEP-RG) and 3 μg/ml α-factor. Fresh α-factor was added to 2 μg/ml after another hour and cultures shifted to 37°C when required ([Figure 2G-H](#)). Cells were collected by filtration, washed with YEP-RG, and resuspended in YEP-RG without α-factor.

For arresting strains that express Cdc20 under control of *pMET3* in metaphase, cells were grown at 30°C in methionine-free synthetic dropout medium containing 2% raffinose (–MET-R) to mid-log phase. Cells were collected by filtration, washed with dH₂O, and resuspended to an OD₆₀₀ of 0.2 in YEP containing 2 mM methionine. After 105 min, galactose was added to 2% for TEV protease induction. 4 h after the start of the arrest, cells were released into –MET-R with 2% galactose (–MET-RG). To re-arrest cells in G1 after release from the metaphase arrest, cells were released into –MET-RG containing 3 μg/ml α-factor. Fresh α-factor was added to 2 μg/ml after another hour.

Where indicated, nocodazole was added to 10 μg/ml, phleomycin was added to 10 μg/ml after adjusting the culture medium with 50 mM HEPES-KOH pH 7.5, or rapamycin was added to 20 nM (liquid cultures) or 100 nM (plates).

Long-term live cell imaging. Cells were loaded for 7 sec at 4 psi into an Onix (CellASIC) microfluidic system mounted on a DeltaVision microscope after equilibrating the system with –MET-R for 3 min at 8 psi. Cells that had not been trapped were removed by washing the chamber for 5 min at 5 psi with –MET-R. Loading and washing steps were repeated until a sufficient number of cells had been trapped. Cells were then synchronized in metaphase by using –MET-R containing 2 mM methionine as flow medium for 90 min at 0.5 psi. TEV protease expression was induced by switching the medium to –MET-RG containing 2 mM methionine for 180 min at 0.5 psi. Single-section transmission images pictures were taken every 5 min during the arrest. Cells were then released into –MET-RG without methionine for 12 h at 0.5 psi. 10 z-sections with 700 nm step size and 0.1 s exposure times at 10% transmission of the GFP filter and single-section transmission images were recorded every 20 min after the release.

FACScan analysis. Cells were collected by centrifugation, washed once with PBS, and fixed with 70% (v/v) ethanol overnight. After fixation, cells were washed with 50 mM sodium citrate pH 7.5 and treated for 1 h with 0.25 mg/ml RNase A and for 1 h with 1 mg/ml proteinase K in 50 mM sodium citrate pH 7.5 at 50°C. Cells were stained for at least 30 min by addition of SYBR green I (1:500, Invitrogen). Before analysis in a FACScan flow cytometer (Becton Dickinson), Triton X-100 was added to 0.25% and samples were sonicated. 10,000 events were acquired with CellQuest (Becton Dickinson) and analyzed with FlowJo (TreeStar).

Immunofluorescence imaging and immunoblotting. For immunofluorescence, cells were fixed at room temperature in formaldehyde for at least 12.25 h and processed as described ([Roberts et al., 1991](#)). In brief, spheroplasts were permeabilized by a short incubation in 1% SDS, 1.2 M sorbitol and then stained with TAT1 α-tubulin antibody ([Woods et al., 1989](#)) and Alexa594-conjugated α-mouse IgG antibody (Invitrogen). Cells were mounted in ProLong Gold AntiFade reagent with DAPI (Invitrogen). For immunoblotting, proteins were separated on 10% SDS PAGE. After semi-dry transfer to PVDF membranes, HA-tagged proteins were detected with monoclonal (12CA5) or polyclonal (ab9110, abcam) anti-HA and peroxidase-conjugated antibodies.

Yeast genotypes.

- C2513** MAT α , Δ brn1::HIS3, ura3::BRN1-HA₆::URA3, pGAL1-NLS-myc₉-TEVprotease-NLS₂::TRP1, leu2::tetR-GFP::LEU2, 2 \times tetO₂₂₄::URA3 integrated between BMH1 and PDA1, cdc20::pMET3-CDC20::LEU2
- C2618** MAT α , Δ brn1::HIS3, ura3::BRN1(3 \times TEV₆₂₂)-HA₆::URA3, pGAL1-NLS-myc₉-TEVprotease-NLS₂::TRP1, leu2::tetR-GFP::LEU2, 2 \times tetO₂₂₄::URA3 integrated between BMH1 and PDA1, cdc20::pMET3-CDC20::LEU2
- C3099** MAT α , Δ brn1::HIS3, ura3::BRN1(3 \times TEV₆₂₂)-HA₆::URA3, pGAL1-NLS-myc₉-TEVprotease-NLS₂::TRP1, cdc20::pMET3-CDC20::TRP1, leu2::pGAL1-FLAG-EosFP::LEU2
- C3100** MAT α , Δ brn1::HIS3, ura3::BRN1-HA₆::URA3, pGAL1-NLS-myc₉-TEVprotease-NLS₂::TRP1, cdc20::cdc20::pMET3-CDC20::TRP1, leu2::pGAL1-FLAG-EosFP::LEU2
- C3144** MAT α , leu2::pGAL1-SCC1(R180D, R268D)-HA₃::LEU2, ura3::pGAL1-FLAG-EosFP::URA3
- C3145** MAT α , top2-4, leu2::pGAL1-FLAG-EosFP::LEU2
- C3233** MAT α , Δ brn1::HIS3, ura3::BRN1-HA₆::URA3, pGAL1-NLS-myc₉-TEVprotease-NLS₂::TRP1, leu2::pGAL1-FLAG-EosFP::LEU2
- C3246** MAT α , Δ brn1::HIS3, ura3::BRN1(3 \times TEV₆₂₂)-HA₆::URA3, pGAL1-NLS-myc₉-TEVprotease-NLS₂::TRP1, leu2::pGAL1-FLAG-EosFP::LEU2
- C3257** MAT α , Δ brn1::HIS3, ura3::BRN1-HA₆::URA3, leu2::pGAL1-NLS-myc₉-TEVprotease-NLS₂::LEU2, trp1::pTUB1-GFP-TUB1::TRP1, cdc20::pMET3-CDC20::LEU2
- C3258** MAT α , Δ brn1::HIS3, ura3::BRN1(3 \times TEV₆₂₂)-HA₆::URA3, leu2::pGAL1-NLS-myc₉-TEVprotease-NLS₂::LEU2, trp1::pTUB1-GFP-TUB1::TRP1, cdc20::pMET3-CDC20::LEU2
- C3279** MAT α , Δ mad2::URA3, Δ brn1::HIS3, ura3::BRN1-HA₆::URA3, leu2::pGAL1-NLS-myc₉-TEVprotease-NLS₂::LEU2, trp1::pTUB1-GFP-TUB1::TRP1, cdc20::pMET3-CDC20::LEU2
- C3280** MAT α , Δ mad2::URA3, Δ brn1::HIS3, ura3::BRN1(3 \times TEV₆₂₂)-HA₆::URA3, leu2::pGAL1-NLS-myc₉-TEVprotease-NLS₂::LEU2, trp1::pTUB1-GFP-TUB1::TRP1, cdc20::pMET3-CDC20::LEU2
- C3294** MAT α , Δ brn1::HIS3, ura3::BRN1-HA₆::URA3, pGAL1-NLS-myc₉-TEVprotease-NLS₂::TRP1, RAD52-GFP::kanMX6
- C3308** MAT α , Δ brn1::HIS3, ura3::BRN1-HA₆::URA3, trp1::cdc20::pMET3-CDC20::TRP1, pGAL1-NLS-myc₉-TEVprotease-NLS₂::TRP1, RAD52-GFP::kanMX6
- C3310** MAT α , Δ brn1::HIS3, ura3::BRN1(3 \times TEV₆₂₂)-HA₆::URA3, trp1::cdc20::pMET3-CDC20::TRP1, pGAL1-NLS-myc₉-TEVprotease-NLS₂::TRP1, RAD52-GFP::kanMX6
- C3372** MAT α , Δ brn1::HIS3, ura3::BRN1(FKBP12₂-TEV₃₆₃-FRB₂)-HA₆::URA3, pGAL1-NLS-myc₉-TEVprotease-NLS₂::TRP1, Δ fpr1::natMX4, Δ TOR1-1
- C3378** MAT α , Δ brn1::HIS3, ura3::BRN1-HA₆::URA3, pGAL1-NLS-myc₉-TEVprotease-NLS₂::TRP1, Δ fpr1::natMX4, TOR1-1
- C3380** MAT α , Δ brn1::HIS3, ura3::BRN1(3 \times TEV₆₂₂)-HA₆::URA3, trp1::pGAL1-NLS-myc₉-TEVprotease-NLS₂::TRP1, cdc20::pMET3-CDC20::TRP1, MRE11-GFP::kanMX6
- C3381** MAT α , Δ brn1::HIS3, ura3::BRN1(3 \times TEV₆₂₂)-HA₆::URA3, pGAL1-NLS-myc₉-TEVprotease-NLS₂::TRP1, MRE11-GFP::kanMX6
- C3382** MAT α , Δ brn1::HIS3, ura3::BRN1-HA₆::URA3, pGAL1-NLS-myc₉-TEVprotease-NLS₂::TRP1, cdc20::pMET3-CDC20::TRP1, MRE11-GFP::kanMX6
- C3432** MAT α , cdc15-2, Δ brn1::HIS3, ura3::BRN1(3 \times TEV₆₂₂)-HA₆::URA3, trp1::pGAL1-NLS-myc₉-TEVprotease-NLS₂::TRP1, MRE11-GFP::kanMX6
- C3434** MAT α , cdc15-2, Δ brn1::HIS3, ura3::BRN1-HA₆::URA3, trp1::pGAL1-NLS-myc₉-TEVprotease-NLS₂::TRP1, MRE11-GFP::kanMX6
- C3467** MAT α , Δ rad9::TRP1, Δ brn1::HIS3, ura3::BRN1-HA₆::URA3, leu2::pGAL1-NLS-myc₉-TEVprotease-NLS₂::LEU2, trp1::pTUB1-GFP-TUB1::TRP1, cdc20::pMET3-CDC20::LEU2
- C3512** MAT α , Δ rad9::TRP1, Δ brn1::HIS3, ura3::BRN1(3 \times TEV₆₂₂)-HA₆::URA3, leu2::pGAL1-NLS-myc₉-TEVprotease-NLS₂::LEU2, trp1::pTUB1-GFP-TUB1::TRP1, cdc20::pMET3-CDC20::LEU2
- C3572** MAT α , Δ brn1::HIS3, ura3::BRN1(FKBP12₂-TEV₃₆₃-Glinker-FRB₂)-HA₆::URA3, pGAL1-NLS-myc₉-TEVprotease-NLS₂::TRP1, leu2::tetR-GFP::LEU2, 2 \times tetO₂₂₄::URA3 integrated between BMH1 and PDA1, Δ fpr1::natMX4, TOR1-1
- C3574** MAT α , Δ brn1::HIS3, ura3::BRN1(FKBP12₂-TEV₆₂₂-Glinker-FRB₂)-HA₆::URA3, pGAL1-NLS-myc₉-TEVprotease-NLS₂::TRP1, leu2::tetR-GFP::LEU2, 2 \times tetO₂₂₄::URA3 integrated between BMH1 and PDA1, Δ fpr1::natMX4, TOR1-1

- C3629** MAT α , Δ brn1::HIS3, ura3::BRN1(FKBP12₂-TEV₆₂₂-GLlinker-FRB₂)-HA₆::URA3, pGAL1-NLS-myc₉-TEVprotease-NLS₂::TRP1, leu2::tetR-GFP::LEU2, 2 \times tetO₂₂₄::URA3 integrated between BMH1 and PDA1, Δ fpr1::natMX4, TOR1-1, cdc20::pMET3-CDC20::LEU2
- C3671** MAT α , Δ brn1::HIS3, ura3::BRN1(FKBP12₂-non-cleavable-linker₆₂₂-FRB₂)-HA₆::URA3, pGAL1-NLS-myc₉-TEVprotease-NLS₂::TRP1, leu2::tetR-GFP::LEU2, 2 \times tetO₂₂₄::URA3 integrated between BMH1 and PDA1, Δ fpr1::natMX4, TOR1-1
- C3696** MAT α , Δ brn1::HIS3, ura3::BRN1(FKBP12₂-non-cleavable-linker₆₂₂-FRB₂)-HA₆::URA3, pGAL1-NLS-myc₉-TEVprotease-NLS₂::TRP1, leu2::tetR-GFP::LEU2, 2 \times tetO₂₂₄::URA3 integrated between BMH1 and PDA1, Δ fpr1::natMX4, TOR1-1, cdc20::pMET3-CDC20::LEU2
- C3796** MAT α , Δ brn1::HIS3, ura3::BRN1-HA₆::URA3, trp1::pGAL1-NLS-myc₉-TEVprotease-NLS₂::TRP1, MRE11-GFP::kanMX6, cdc12-6
- C3801** MAT α , Δ brn1::HIS3, ura3::BRN1(3 \times TEV₆₂₂)-HA₆::URA3, trp1::pGAL1-NLS-myc₉-TEVprotease-NLS₂::TRP1, MRE11-GFP::kanMX6, cdc12-6
- C3873** MAT α , Δ brn1::HIS3, ura3::BRN1-HA₆::URA3, leu2::pGAL-NLS-myc₉-TEVprotease-NLS₂::LEU2, trp1::pTUB1-GFP-TUB1::TRP1, cdc20::pMET3-CDC20::LEU2, Δ yku70::kanMX4
- C3874** MAT α , Δ brn1::HIS3, ura3::BRN1(3 \times TEV₆₂₂)-HA₆::URA3, leu2::pGAL-NLS-myc₉-TEVprotease-NLS₂::LEU2, trp1::pTUB1-GFP-TUB1::TRP1, cdc20::pMET3-CDC20::LEU2, Δ yku70::kanMX4
- C3875** MAT α , Δ brn1::HIS3, ura3::BRN1(3 \times TEV₆₂₂)-HA₆::URA3, leu2::pGAL-NLS-myc₉-TEVprotease-NLS₂::LEU2, trp1::pTUB1-GFP-TUB1::TRP1, cdc20::pMET3-CDC20::LEU2, MYO1-mCherry₃::kanMX6
- C3877** MAT α , Δ brn1::HIS3, ura3::BRN1-HA₆::URA3, leu2::pGAL-NLS-myc₉-TEVprotease-NLS₂::LEU2, trp1::pTUB1-GFP-TUB1::TRP1, cdc20::pMET3-CDC20::LEU2, CHS2-mCherry₃::kanMX6
- C3898** MAT α , Δ brn1::HIS3, ura3::BRN1-HA₆::URA3, leu2::pGAL-NLS-myc₉-TEVprotease-NLS₂::LEU2, trp1::pTUB1-GFP-TUB1::TRP1, cdc20::pMET3-CDC20::LEU2, MYO1-mCherry₃::kanMX6
- C3899** MAT α , Δ brn1::HIS3, ura3::BRN1(3 \times TEV₆₂₂)-HA₆::URA3, leu2::pGAL-NLS-myc₉-TEVprotease-NLS₂::LEU2, trp1::pTUB1-GFP-TUB1::TRP1, cdc20::pMET3-CDC20::LEU2, CHS2-mCherry₃::kanMX6

SUPPLEMENTAL REFERENCES

- Roberts, C.J., Raymond, C.K., Yamashiro, C.T., and Stevens, T.H. (1991). Methods for studying the yeast vacuole. *Meth Enzymol* 194, 644–661.
- Woods, A., Sherwin, T., Sasse, R., MacRae, T.H., Baines, A.J., and Gull, K. (1989). Definition of individual components within the cytoskeleton of *Trypanosoma brucei* by a library of monoclonal antibodies. *J Cell Sci* 93, 491–500.